Experimental and Theoretical Study on the Flexural Enhancement of Rice Sack Waste FRP-strengthened RC Beams

A. Honestyo[1], Tavio[1*], H. Ardhyananta[2]

[1]Department of Civil Engineering, Institut Teknologi Sepuluh Nopember, Surabaya, 60111, Indonesia.
[2]Department of Materials and Metallurgical Engineering, Institut Teknologi Sepuluh Nopember, Surabaya 60111, Indonesia

ABSTRACT: Reinforced concrete beams deteriorate over time due to design errors, substandard materials, improper construction practices, overloading, and long-term effects such as creep and shrinkage. Fibre-reinforced plastic (FRP) is widely used for strengthening, but its production raises environmental concerns. Meanwhile, plastic waste such as rice sacks is increasingly abundant in Indonesia and offers potential as a sustainable fibre material. This study explores the use of rice sack waste–based FRP composites for flexural strengthening of reinforced concrete beams. Beams were externally bonded with varying numbers of FRP layers, and their performance was evaluated through experimental flexural testing and theoretical predictions using ACI 440.2R-17. The results demonstrate that the waste-based FRP composites can enhance beam capacity, with effectiveness influenced by the number of layers applied. While ACI 440.2R-17 successfully predicts the general strengthening trend, it consistently overestimates the actual capacity observed in experiments. These findings indicate that the guideline is useful as a reference but requires refinement to better capture the behaviour of sustainable FRP composites in practical applications.

KEYWORDS: Composite, Disaster Risk Reduction, FRP, Reinforced Concrete Beams, Rice Sack Waste.

[Received Nov. 29, 2024; Revised June 16, 2025; Accepted July 19, 2025] Print ISSN: 0189-9546 | Online ISSN: 2437-2110

I. INTRODUCTION

To obtain optimal performance from a building, its structural members must be carefully designed based on applicable regulations, including proper implementation in the construction process (Agustiar et al., 2018; Anggraini et al., 2018, 2021; Wahjudi, 2014). Many materials are often used to reinforce or strengthen structural members, such as steel plates and non-metallic materials (Machmoed and Raka, 2020, 2021; Sabariman et al., 2020; Tavio et al., 2021, 2022; Rafani et al., 2021).

Reinforced concrete beams or columns deteriorate over time due to various factors, such as design and calculation errors, the use of substandard materials, improper installation practices, overloading beyond permissible limits, and long-term effects such as creep and shrinkage cracking in the concrete. These cracks allow water to infiltrate the structural members, which may lead to corrosion (Jung et al., 2019). To address this issue, reinforced concrete beams or columns must be strengthened to restore their original capacity. Such strengthening efforts typically improve the beam or column's load-bearing capacity and extend its overall service life (Raval and Dave, 2013; Pinto et al., 2019).

Several methods are commonly used to enhance the performance of reinforced concrete beams or columns, one of which is external reinforcement. This includes the use of steel plates, external steel bars, and fibre-reinforced polymer (FRP) materials (Aykac et al., 2013; Honestyo et al., 2023a). However, steel plates and bars are vulnerable to environmental exposure, as they oxidize easily and are prone to corrosion (Jung et al., 2019). Their use is not recommended for long-term applications, as they require periodic replacement when corrosion occurs.

Fibre-reinforced polymer (FRP) is a composite material typically composed of two main constituents: a fibre phase and a matrix. FRP is more resistant to corrosion than traditional materials, making it more economical due to its extended service life and reduced maintenance requirements (Darain et al., 2016). The fibres used in FRP are often synthetic, including glass, aramid, carbon, and basalt fibres. Previous studies have demonstrated that synthetic FRP can effectively enhance the flexural strength, stiffness, and deflection behaviour of reinforced concrete beams. These studies have investigated various FRP parameters such as mechanical properties, spacing, dimensions, configurations, and the number of layers (Abdel-Jaber et al., 2007).

Al-Tamimi et al. (2011) y investigated the use of different FRP configurations to improve the flexural capacity of reinforced concrete beams. The results showed a 65% increase in bending strength compared to the control group. The study highlighted several influencing factors, including the reinforcement ratio, number of FRP layers, and FRP dimensions. It was found that applying FRP to at least 25% of the beam span significantly improved performance, resulting in an average increase of approximately 80% in flexural capacity. In another study, Carbon Fibre Reinforced Polymer

*Corresponding author: tavio@its.ac.id

doi: http://doi.org/10.63746/njtd.v22i4.3131

(CFRP) sheets applied to the tension face of reinforced concrete beams improved flexural performance, with increases ranging from 41% to 125%, depending on beam geometry, loading conditions, and the CFRP application method (Dong et al., 2013).

Further research on reinforced concrete beams strengthened with CFRP sheets and laminates revealed that increasing the number of FRP layers significantly improved load-bearing capacity in both vertical and horizontal orientations. The maximum observed increase in bending strength was found by Al-Ghanim et al. (2017) to be 51%. In addition, applying laminate strips along the full length of the beam between supports led to a 26% increase in flexural strength, while narrower strip widths only produced a 9% improvement, indicating the importance of strip dimensions in achieving effective reinforcement.

However, many synthetic FRP materials currently used for beam strengthening are considered environmentally unfriendly. Their long-term use can negatively affect both biotic and abiotic components of the ecosystem. The production of synthetic fibres involves excessive resource extraction, air pollution, and contributes to greenhouse gas emissions. As such, alternative, eco-friendly fibre materials for FRP development are urgently needed.

One promising alternative is the use of plastic waste as the fibre phase in FRP production. For instance, FRP made with PET fibres has demonstrated a tensile strength of up to 65 MPa (Honestyo et al., 2023b), proving its viability as a reinforcing material. Moreover, FRP made from recycled plastic fibres has shown potential for use as external reinforcement in structural applications.

In Indonesia, one of the world's largest rice-producing countries, rice sacks are a common form of plastic waste. These sacks are typically made from woven plastic fibres and are often discarded after use. Once disposed of, they contribute to environmental problems such as waterlogging and serve as breeding grounds for mosquitoes, particularly those that transmit dengue fever. Plastic pollution is a major global issue. Each year, an estimated 19–23 million tons of plastic waste enter the environment (Borrelle et al., 2020). The accumulation of plastic waste in sediments has even become a geological marker of the Anthropocene (Brandon et al., 2019).

Plastic waste presents several major challenges: (1) it accounts for approximately one-third of environmentally harmful waste (Ritch et al., 2009); (2) it breaks down into microplastics, which enter the food chain and cause further ecological harm (Rocha-Santos and Duarte, 2009); and (3) it is difficult to recycle and often ends up in landfills (O'Farrel, 2018). Rice sacks, like other plastic waste, follow a similar path and contribute to these growing concerns.

To address both environmental pollution and the structural degradation of reinforced concrete beams, this study proposes the use of plastic waste from rice sacks as the fibre component in the development of FRP for external reinforcement. The first phase involves determining the optimal fibre-to-matrix ratio to achieve the best tensile strength performance. The resulting FRP was then applied as external strengthening for concrete beams. Experimental results were then compared with theoretical predictions based on ACI 440.2R-17.

Despite the proven effectiveness of synthetic FRP in enhancing the flexural performance of reinforced concrete beams, concerns remain regarding its long-term environmental impact. The extensive use of non-biodegradable and resource-intensive materials in conventional FRP production has prompted the need for more sustainable alternatives. However, research on eco-friendly FRP, particularly those incorporating post-consumer plastic waste such as rice sacks, remains limited. This study addresses this gap by investigating the feasibility of using plastic rice sacks as the fibre phase in FRP composites for beam strengthening. The primary objective is to evaluate the mechanical performance of this alternative FRP through experimental and theoretical approaches, thereby contributing to the development of greener solutions in structural retrofitting.

Chapter I introduces the study background, literature review, and research objectives. Chapter II outlines the experimental program, including materials and test setup. Chapter III presents the theoretical analysis based on ACI 440.2R-17 to predict the flexural behaviour of the beams. Chapter IV provides the results and discussion, comparing experimental outcomes with theoretical models. Finally, Chapter V concludes the study by summarizing the key findings.

II. EXPERIMENTAL PROGRAM

The rice sacks were collected as household waste. They were then cleaned using an antiseptic solution, rinsed with running water, and dried. The rice sacks served as the fibre phase, while a commercial resin acted as the matrix phase. These two components were combined in a 1:1 density ratio to produce the composite FRP, as illustrated in Figure 1. Figure 1(b) shows two samples with fibre orientation of 0 and 90 degrees (top), and 45 degrees (bottom), respectively. In this study, a fibre orientation of 45 degrees was selected, as this angle has been found to provide higher tensile strength. The mechanical properties of the resulting FRP were determined using the ASTM D3039 tensile test, with the results summarized in Table 1.

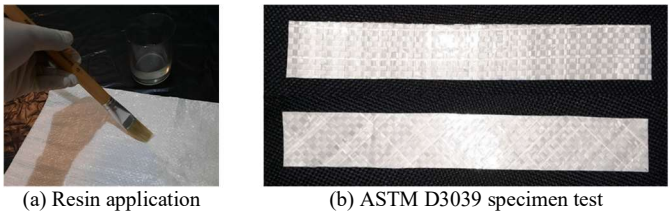

(a) Resin application (b) ASTM D3039 specimen test

Figure 1. FRP composite used in this study

Table 1. Typical properties of composite FRP used

Elastic modulus (GPa)	7.6
Elastic tensile strength (MPa)	38.7
Elastic tensile strain (mm/mm)	0.005
Rupture tensile strength (MPa)	61.2
Rupture tensile strain (mm/mm)	0.04

Six concrete cylinders were prepared for compressive strength testing, yielding an average value of 17 MPa at 28 days. The flexural reinforcement used in the concrete beams consisted of 10 mm diameter steel bars with an average yield strength of 400 MPa, an ultimate strength of 680 MPa, and an elastic modulus of 200 GPa. The reinforced concrete beams were designed to undergo tension, with a target yield strain of 0.008 to ensure sufficient ductility and to allow for visible signs of distress prior to failure, as illustrated in Figure 2.

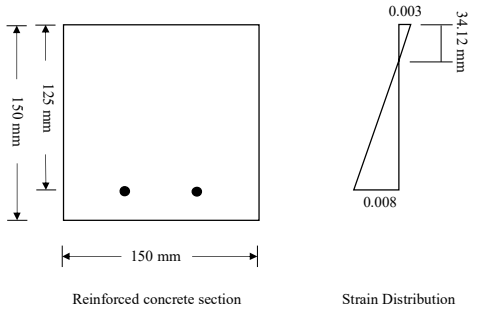

Figure 2. Reinforced concrete beam designated under tension

The beam span was designed in accordance with ASTM C78, with an overall length of 500 mm and a cross-sectional dimension of 150 mm × 150 mm, as shown in Figure 3. Experimental testing was conducted on reinforced concrete beams strengthened with FRP applied in three different layer configurations. The beams were labelled as follows: BF1 for beams with one layer of FRP (3 mm), BF2 with two layers (6 mm), and BF3 with three layers (9 mm) (Figure 4). Each configuration consisted of three specimens, resulting in a total of nine beam specimens.

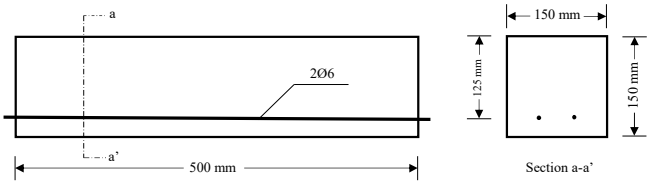

Figure 3. Reinforced concrete beam span and configuration

The FRP composite was applied directly to the tension face of the concrete beams using the hand lay-up method. Prior to application, the beam surfaces were smoothed using sandpaper to remove dust and loose particles, then cleaned with water and dried using a towel. To further improve bonding quality between the FRP and the concrete substrate, additional roughening was performed using a wire brush to enhance mechanical interlocking and adhesion.

During the lay-up process, resin was applied to both the beam surface and the rice sack fibre layer. Manual pressure using a roller was used to eliminate air pockets and ensure proper fibre wetting and contact. The fibres were laid in a unidirectional pattern and oriented at 45 degrees, using visual guides marked on the beam surface to maintain consistent alignment across all specimens. The configuration of the FRP-strengthened beams is illustrated in Figure 4.

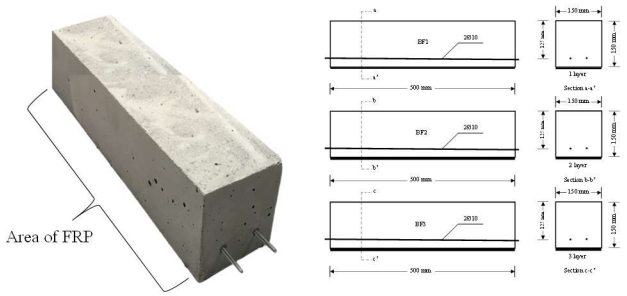

Figure 4. FRP-strengthened RC beam configuration with one, two, and three layers

To ensure repeatability, all specimens underwent the same surface preparation, fibre orientation, and resin application procedures. No visible signs of debonding or delamination were observed after curing, indicating satisfactory bonding performance across all beams. Flexural tests were carried out using a three-point bending setup, with a constant load rate of 10 kN/min. The beams were simply supported with a span length of 450 mm, using steel rods to simulate pinned and roller supports as shown in Figure 5.

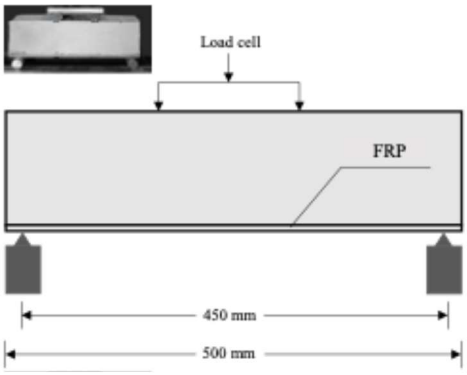

Figure 5. Flexural test set up

III. THEORITICAL PROGRAM

To calculate the flexural capacity of reinforced concrete beams, this study adheres to the ACI 440.2R-17 standards for external FRP systems (ACI 440.2R, 2017). The following section provides the code formulas and constraints for determining the flexural capacity of beams reinforced with FRP materials. The ultimate load-bearing capacity of FRP-strengthened reinforced concrete beams in bending can be estimated through compatibility of strain (Eq. 1) and equilibrium of force (Eq. 2). Figure 6 illustrates the stress-strain distribution of concrete beam strengthened by FRP at the level of ultimate limit. Here, α_1 denotes the factor applied to f_c' tnb o obtain the concrete equivalent rectangular stress distribution, β_1 is the ratio of the rectangular stress sections equivalent depth to the neutral axis, A_s is the area of FRP external strengthening.

$$\alpha_1 f_c' \beta_1 bc = A_s f_s + A_f f_{fe} \quad (1)$$

$$M_n = A_s f_s (d - \beta_1 \frac{c}{2}) + \psi_f A_f f_{fe} (d_f - \beta_1 \frac{c}{2}) \quad (2)$$

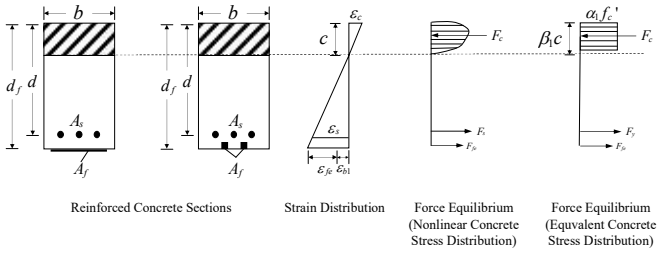

Figure 6. Internal stress and strain distribution (ACI 440.2R, 2017)

The flexural strength design of the FRP-strengthened reinforced concrete beam (φM_n), following the guidelines of ACI 440.2R-17, it can be calculated by combining the input of flexural from the external FRP (M_{nf}) with that from the internal steel reinforcement (M_{ns}) as shown in Equation 3. An additional reduction factor, ψ_f, is introduced to adjust the flexural strength prediction for reliability and to account for the various failure modes observed in FRP-strengthened structural members. ACI 440.2R-17 recommends setting the value of ψ_f to 0.85. Furthermore φ represents the factor of strength reduction for flexure which ensures sufficient ductility, with value of 0.9. To prevent intermediate crack-induced debonding failure, the effective strain in the FRP strengthening ε_{fd} must be limited, as specified in ACI 440.2R-17, Section 10.1, and illustrated in Equation 4. In this equation, n represents the number of FRP layers, t_f is the thickness of the layer, E_f is the elastic modulus, and ε_f is the design rupture strain in FRP.

$$\varphi M_n = \varphi \left[M_{ns} + \psi_f M_{nf} \right] \quad (3)$$

$$\varepsilon_{fd} = 0.41 \sqrt{\frac{f_c'}{nE_f t_f}} \leq 0.9 \varepsilon_f \quad (4)$$

According to ACI 440.2R-17, determining the ultimate strength of reinforced concrete beams that have been strengthened in flexure follows an iterative procedure. This approach ensures accuracy and accounts for the complex interactions between the materials and structural elements. The process begins with an initial assumption of the depth to the neutral axis, which serves as the starting point for further calculations (c). Following this, the strain in each material of concrete, steel reinforcement, and FRP is determined using strain compatibility equations, which are crucial for ensuring that the deformations in the materials are compatible with each other under load. Once the strains are calculated, the corresponding stresses in each material are computed, using the material properties and the strain values obtained. The next step in the process is to verify the equilibrium of internal forces. This step ensures that the total internal forces, including the contributions from the concrete, steel reinforcement, and FRP, balance out in the system. If an imbalance is detected, the length to the neutral axis must be adjusted accordingly, and the entire process is repeated with the updated value. This iterative process continues until equilibrium is achieved, and the correct values for strain, stress, and the neutral axis depth are obtained. To model the behaviour of the FRP material in the system, ACI 440.2R-17 provides the equations for the effective strain of the limit level (ε_{fe}) and the stress of FRP (f_{fe}), assuming with the behaviour of perfectly elastic. These values are essential in accurately assessing the contribution of the FRP to the beam's overall strength. Specifically, Equation 5 provides the calculation for the effective strain at the limit state, while Equation 6 determines the stress in the FRP. In this equation ε_c represents the concrete strain, d_f is the FRP effective depth, and ε_{bi} is concrete substrate strain at time when FRP was installed.

$$\varepsilon_{fe} = \varepsilon_{cu} \frac{d_f - c}{c} - \varepsilon_{bi} \leq \varepsilon_{fd} \quad (5)$$

$$f_{fe} = E_f \varepsilon_{fe} \quad (6)$$

Longitudinal reinforcement strain (ε_s) is computed based on the FRP strengthening effective strain, employing the strain compatibility method, as outlined in Equation 7. This method ensures that the strains in the materials are consistent and compatible under loading, which is crucial for an accurate assessment of the beam's behaviour. The FRP effective strain is derived by considering the deformation in both the FRP material and the concrete substrate. Once the strain of the FRP is established, the strain of the longitudinal reinforcement is computed accordingly, ensuring compatibility between the materials involved in the strengthening process. Next, the corresponding stress of the existing steel reinforcement (f_s) is obtained from the steel strain, using the assumption as described in Equation 8. This approach assumes that the steel reinforcement behaves elastically up to a certain yield point, after which it exhibits perfectly plastic behaviour. The yield stress is determined based on the material properties of the steel, and the stress is calculated accordingly. This simplification allows for an efficient calculation while still accurately representing the behaviour of the steel reinforcement under typical loading conditions. The nominal flexural strength components of the reinforced concrete beams, which include the contributions from both the steel reinforcement and the FRP strengthening, are determined using Equations 9 and 10. These equations consider the moment capacities of each material, the collaboration between the reinforcement of steel and FRP, and the overall cross-sectional properties of the beam. By considering the individual strengths of the materials and their interaction, these equations provide a comprehensive evaluation of the beam's total flexural strength. The nominal flexural strength is critical for ensuring that the beam meets design requirements, including safety margins and performance under expected service loads. Together, these calculations provide a complete and accurate assessment of the

ultimate flexural strength of the reinforced concrete beam, considering the contributions of both the traditional steel reinforcement and the externally applied FRP strengthening. This iterative process ensures that the design is robust, with a clear understanding of how the beam may perform under various loading conditions.

$$\varepsilon_s = \left(\varepsilon_{fe} + \varepsilon_{bi}\right)\frac{d-c}{d_f - c} \tag{7}$$

$$f_s = E_s\varepsilon_s \le f_y \tag{8}$$

$$M_{ns} = A_s f_s\left(d - \frac{\beta_1 c}{2}\right) \tag{9}$$

$$M_{nf} = A_f f_{fe}\left(d_f - \frac{\beta_1 c}{2}\right) \tag{10}$$

IV. RESULTS AND DISCUSSION

A. Theoretical Results

The theoretical predictions for the control beams were made following the guidelines provided in ACI 318-19, which offers comprehensive standards for the design and analysis of reinforced concrete structures. ACI 318-19 outlines the procedures for determining the flexural strength of non-strengthened beams, based on factors such as the beam's geometry, material properties, and the amount of reinforcement. In contrast, the flexural loads for the FRP-strengthened beams were estimated using ACI 440.2R-17, which is specifically focused on the design and strengthening of concrete structures with FRP strengthening. ACI 440.2R-17 provides detailed procedures for calculating the flexural capacity of reinforced concrete beams that are externally strengthened with FRP materials. This standard considers the contribution of the FRP to the overall strength of the beam, as well as the interaction between the FRP and the original concrete and steel reinforcement. By applying the methodologies outlined in ACI 440.2R-17, the impact of the FRP on the capacity at ultimate load-carrying of the beams can be accurately predicted. To determine the capacity at ultimate load-carrying of the FRP-strengthened reinforced concrete beams in flexure, two key methods are used: strain compatibility and force equilibrium. Strain compatibility, as defined in Equation 1, confirms that the strains in the various materials—concrete, steel reinforcement, and FRP—are consistent under loading. This method accounts for the fact that all materials in the beam deform together, and their strains must be compatible to achieve a realistic assessment of the beam's behaviour. By using strain compatibility, the effective strain of FRP, steel reinforcement, and concrete can be determined, allowing for a comprehensive evaluation of the beam's response to bending. Force equilibrium, described in Equation 2, ensures that the internal forces within the beam are balanced. This equation considers the forces generated by the concrete, the steel reinforcement, and the FRP material, and requires that the sum of these forces equals zero for the beam to be in a state of equilibrium. If the internal forces do not balance, adjustments must be made to the assumed parameters (such as the neutral axis depth) and the calculations are repeated until equilibrium is achieved. The force equilibrium method is crucial for determining the actual load-carrying capacity of the beam, as it accounts for the interaction of all materials and forces within the system. These equations are used to calculate the stress and strain distributions for each specimen, as shown in Figure 7. Figure 7 illustrates that all the reinforcement in the beam has yielded $\left(\varepsilon_s > \varepsilon_y\right)$, meaning the addition of three layers of FRP does not cause the reinforced concrete to become over-reinforced. Additionally, FRP has reached its ultimate strain at the limit state $\left(\varepsilon_{fe} = 0.0045\right)$, and the strain of concrete substrate at time of FRP installation. (ε_{bi}) decreases as the number of FRP layers increases.

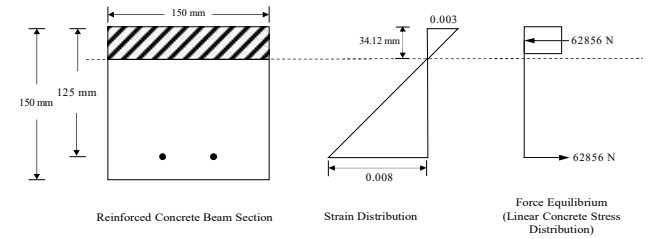

(a) Control specimen

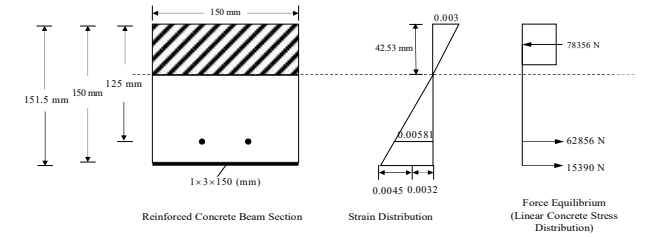

(b) BF1 specimen

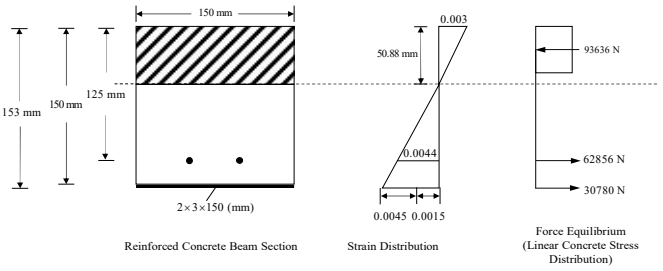

(c) BF2 specimen

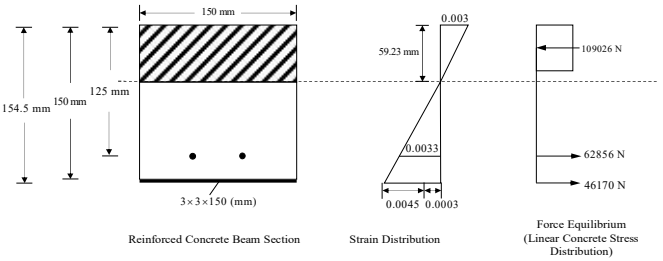

(d) BF3 specimen

Figure 7. Internal stress and strain distribution of the specimens

Using force equilibrium, as outlined in Figure 7, the nominal flexural strength capacity of each specimen can be determined with the help of Equations 9 and 10. Table 2 presents the nominal flexural strength capacity for each specimen, illustrating the impact of Fiber Reinforced Polymer (FRP) layers on the moment capacity. The addition of FRP layers results in a notable increase in nominal moment capacity. Specifically, the use of one layer (BF1) enhances the capacity by 26% compared to the control specimen. When two layers of FRP are applied (BF2), the capacity increases by an additional 20% compared to BF1. Further increasing to three layers (BF3) results in a 16% increase in capacity over BF2. By applying the simple beam theory shown in Figure 5, along with the nominal flexural strength capacity data from Table 2, the applied load at the ultimate limit state can be determined. The corresponding values of the applied load are presented in Table 3, providing a comprehensive overview of the load distribution at the ultimate condition for each specimen.

Table 2. Nominal flexural strength capacity of reinforced concrete beams

Specimen	M_{ns} (MPa)	M_{nf} (MPa)	$M_n tot$ (MPa)
Control	6945525	-	6945525
BF1	6720862	2053406	8774268
BF2	6497801	4043753	10541554
BF3	6274741	5971039	12245780

Table 3. Failure load capacity of reinforced concrete beams

Specimen	$M_n tot$ (MPa)	Failure load (kN)	Gain in failure load (%)
Control	6945525	92.61	-
BF1	8774268	116.99	26.32
BF2	10541554	140.55	51.77
BF3	12245780	163.28	76.31

B. Experimental Results

The beams were thoroughly examined for crack patterns on their surfaces to identify the first crack load and failure mode, as illustrated in Figure 7. This inspection was essential to understanding the structural performance and behaviour of the beams under loading conditions. The control presented a typical mode of failure, which started with the yielding of the steel. As the load increased, the steel reinforcement reached its yield point, leading to a redistribution of stresses. This was followed by the crushing of concrete in the compression area of the beams, where the concrete could no longer withstand the compressive forces and failed. Flexural cracks, which are characteristic of bending failures, initiated in the tension region of the beams at mid-span and propagated vertically towards the loading point. These cracks typically grew wider as the beam approached failure, indicating a progressive failure mechanism that began in the tensile zone and spread toward the support points.

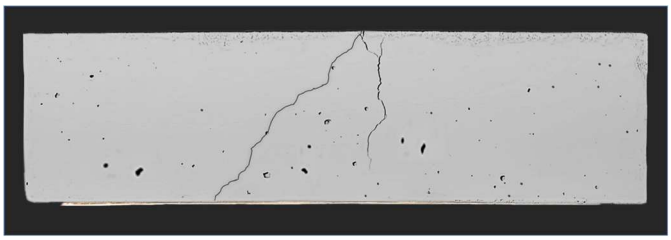

(a) BF1 specimen

(b) BF2 specimen

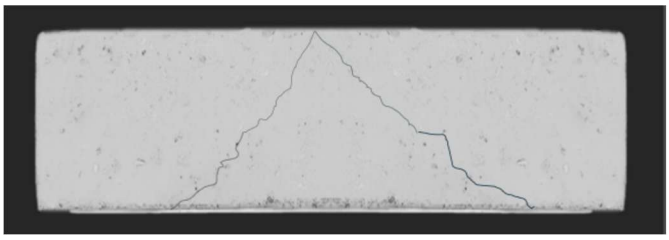

(c) BF3 specimen

Figure 8. Reinforced concrete beams' failure modes

In contrast, the FRP-strengthened reinforced concrete beams (BF1, BF2, and BF3) exhibited similar distinct shifts in failure modes, characterized predominantly by shear failures rather than flexural failures. Diagonal tension cracks were observed forming near the supports and propagating across the beam at an angle, a typical indicator of shear distress with minor debonding only. The addition of FRP reinforcement on the tension face effectively enhanced the flexural capacity of the beams, delaying the onset of flexural cracks and allowing the beams to sustain higher loads in bending. However, this improvement in flexural strength also altered the stress distribution within the beam, inadvertently shifting the critical failure region from mid-span toward the shear spans. As a result, although the beams became stronger in resisting bending moments, they ultimately failed in shear—a more brittle and sudden failure mode compared to flexure. This transition in failure behaviour highlights the importance of considering both flexural and shear capacities when applying FRP strengthening. Without adequate shear reinforcement or additional shear strengthening, the benefits of increased flexural capacity may be offset by premature failure due to shear.

Table 4 presents the test results of the beam specimens, including the load-carrying capacity at first and failure. The

results clearly indicate that all the strengthened beams demonstrated improved performance, with higher loads at both the first and failure, when compared to the controls. This suggests that the flexural strengthening significantly enhanced the beams' load-bearing capacities, providing evidence that the FRP reinforcement effectively contributed to the overall strength and durability of the beams. Specifically, the application of a single layer of FRP to the reinforced concrete beams (designated as BF1) resulted in a 22% increase in the failure load compared to the control specimen. This improvement highlights the benefits of FRP reinforcement in enhancing the flexural strength of the beams. The use of just one layer of FRP seems to provide a substantial enhancement in the beam's load-carrying capacity, demonstrating the effectiveness of even minimal FRP reinforcement in improving structural performance.

Table 4. Flexural test result of reinforced concrete beams

Specimen	First crack load (kN)	Failure load (kN)	Gain in failure load (%)
Control	48.11	73.12	-
BF1	61.07	89.73	22.71
BF2	64.21	104.06	42.31
BF3	63.32	111.76	52.84

For the BF2 specimens, which received additional FRP reinforcement, the failure load increased by 15% compared to the BF1 specimens. This additional increment suggests that the inclusion of multiple layers of FRP further contributes to the beam's strength, although the improvement is less pronounced than the initial increase from BF1. The incremental increase in failure load observed with BF2 may indicate diminishing returns with the additional FRP layers, suggesting that there is a point at which adding more layers of FRP has a reduced effect on increasing the load capacity of the beams. However, for the BF3 specimens, which received the highest level of FRP strengthening, the increase in failure load was only 10% compared to BF2. This relatively smaller improvement could be attributed to several factors, such as the possibility of reaching a saturation point in terms of the FRP's contribution to the beam's strength, or the emergence of other failure modes, such as shear failure or FRP de-bonding, that limit the effectiveness of the additional layers. The results suggest that while increasing the amount of FRP reinforcement does provide a benefit, the incremental improvement in flexural strength may decrease as the level of reinforcement increases beyond a certain threshold. These findings indicate that the use of FRP reinforcement can significantly enhance the flexural strength of reinforced concrete beams, but the rate of improvement varies depending on the number of FRP layers applied. This highlights the importance of optimizing the amount of FRP reinforcement to achieve the desired performance while avoiding unnecessary material use or potential limitations associated with over-reinforcement. The results also emphasize the need for a balanced approach in the design of FRP-strengthened beams, where factors such as cost, material efficiency, and the overall behavior of the beam under loading conditions must be carefully considered.

C. Comparison of Theoretical and Experimental Results

Figure 9 compares the failure load between the theoretical results using ACI 440.2R-17 and the results of experimental testing. Based on the figure, both theoretical and experimental results show the same trend, where the failure load increases with the number of layers. However, the increase in failure load for each additional layer becomes smaller compared to the previous layer.

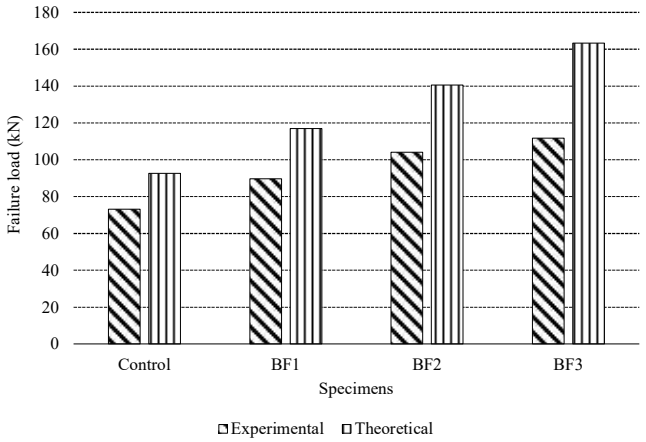

Figure 9. The comparison of failure load

In the experimental testing, the use of one layer of FRP on reinforced concrete beams (BF1) led to a 22% increase in failure load compared to the control specimen. For BF2 and BF3, the increases were 15% and 10%, respectively, relative to the previous FRP configurations. Theoretical predictions based on ACI 440.2R-17, however, indicate a higher enhancement in capacity: 26% for BF1, followed by 20% and 16% for BF2 and BF3, respectively.

While both experimental and theoretical results show a consistent trend of increasing strength with more FRP layers, the absolute values differ considerably. As presented in Table 5, the ACI method consistently overestimates the failure load. The error between theoretical and experimental values increases with the number of FRP layers: from 30% in BF1 to 46% in BF3. Even the control specimen shows a significant error of 27%, indicating that the model may already overpredict capacity before FRP is applied.

Table 5. The comparison of failure load

Specimen	Experimental (kN)	Theoretical (kN)	Error (%)
Control	73.12	92.61	27
BF1	89.73	116.99	30
BF2	104.06	140.55	35
BF3	111.76	163.28	46

Although no major debonding was observed during the tests—only minor separation at the FRP–concrete interface—the rising error cannot be solely attributed to bonding issues. Instead, the increasing discrepancy suggests inherent limitations in the ACI 440.2R-17 model, especially in its assumptions of perfect bonding, uniform strain distribution, and full engagement of all FRP layers in flexural resistance.

Moreover, practical factors such as variability in material properties, imperfect FRP installation (e.g., slight air gaps, resin inconsistencies), and local concrete defects, while often minor, may have cumulative effects that reduce actual performance. Additionally, the diminishing effectiveness of adding more FRP layers in the experimental results implies that outer layers may not be fully activated, possibly due to strain incompatibility or premature microcracking, which are not considered in the ACI approach.

V. CONCLUSION

Rice sack wastes can serve as an alternative fiber reinforcement for composite materials used in the development of reinforced concrete beams. However, the reinforcement capacity achieved is not particularly significant, as the mechanical properties of the composite remain relatively low. Both experimental testing and the theoretical approach using ACI 440.2R-17 indicate that the capacity of the beam increases with the addition of FRP layers. Experimental results show that up to three layers of FRP composite can enhance the beam's capacity by as much as 52%. On the other hand, the theoretical approach suggests that three layers of FRP composite can increase the capacity by up to 76%. While the ACI 440.2R-17 approach is generally effective in predicting trends and providing a general understanding of beam capacity increases, it assumes ideal conditions and does not account for various errors that may occur during specimen fabrication and testing. As a result, the comparison between theoretical and experimental results reveals a significant discrepancy, with error values reaching up to 46% for beams reinforced with three layers of FRP composite. In conclusion, while the ACI 440.2R-17 guidelines provide a useful benchmark for predicting flexural capacity improvements, the growing deviation between theoretical and experimental results, especially with increased FRP usage, highlights the need for cautious application and potential refinement of the model. Incorporating more detailed bond behavior, strain distribution mechanisms, and practical limitations could improve the predictive accuracy of such analytical approaches.

AUTHOR CONTRIBUTIONS

A. Honestyo: Calculation, Experimental, Data analysis and evaluation, original draft preparation, Editing. **Tavio:** Conceptualization, Methodology, Supervision, Review process.

ACKNOWLEDGEMENT(S)

This research was made possible due to financial support from the Directorate of Research, Technology, and Public Services, Ministry of Education and Culture, Research, and Technology of the Republic of Indonesia, and the Directorate of Research and Public Services, Institut Teknologi Sepuluh Nopember (ITS) through Research Grant PMDSU with Contract No: 1454/PKS/ITS/2024. The authors gratefully acknowledge financial support from the Institut Teknologi Sepuluh Nopember for this work, under project scheme of the Publication Writing and IPR Incentive Program (PPHKI) 2025

REFERENCES

Abdel-Jaber, M. S.; A. S. Shatanawi and M. Abdel-Jaber. (2007). Guidelines for shear strengthening of beams using carbon fiber-reinforced polymer (FRP) plates. Jordan Journal of Civil Engineering, 1 (4): 327-335.

ACI 318-19. (2019). Building Code Requirements for Structural Concrete, American Concrete Institute.

ACI 440.2R. (2017). Guide for the Design and Construction of Externally Bonded FRP Systems for Strengthening Concrete Structures, American Concrete Institute.

Agustiar; Raka, I. G. P. and Anggraini, R. (2018). Behavior of concrete columns reinforced and confined by high-strength steel bars. International Journal of Civil Engineering and Technology, 9(7), 1249–1257.

Al-Ghanim, H.; A. Al-Asi; M. Abdel-Jaber; M. Alqam. (2017). Shear and flexural behavior of reinforced concrete deep beams strengthened with CFRP composites. Mod Appl Sci, 10(11): 110-122.

Al-Tamimi, A. K.; R. Hawileh; J. Abdallah and H. A. Garrit. (2011). Effects of ratio of CFRP plate length to shear span and end anchorage on Flexural behavior of SCC RC beams. Journal of composite construction, 15 (6): 908-919.

Anggraini, R.; Raka, I. G. P. and Agustiar. (2021). Flexural capacity of concrete beams reinforced with high-strength steel bars under monotonic loading. International Journal of GEOMATE, 20(77), 173–180.

Anggraini, R.; Raka, I. G. P. and Agustiar. (2018). Stress-strain relationship of high-strength steel (HSS) reinforcing bars. AIP Conference Proceeding, 1964, 020025.

Aykac, S.; I. Kalkan; B. Aykac; S. Karahan and S. Kayar. (2013). Strengthening and repair of reinforced concrete beams using external steel plates. Journal of Structure Engineering, 139: 929-939.

Borrelle, S. B.; J. Ringma; K. L. Law; C. C. Monnahan; L. Lebreton; A. Mcgivern; E. Murphy; J. Jambeck; G. H. Leonard; M. A. Hilleary; M. Eriksen; H. P. Possingham; H. D. Frond; L. R. Gerber; B. Polidro; A. Tahir; M. Bernard; N. Mallos; M. Barnes and C. M. Rochman. (2020). Predicted growth in plastic waste exceeds efforts to mitigate plastic pollution. Science, 369(6540): 1515-1518.

Brandon, J. A.; W. Jones and M. D. Ohman. (2019). Multidecadal increase in plastic particles in coastal ocean sediments. Science Advances, 5(9):1-5.

Darain, Kh M.u.; M.Z. Jumaat; A. A. Shukri; M. Obaydullah; Md N. Huda; MdA. Hosen and N. Hoque. (2016). Strengthening of RC beams using externally bonded reinforcement combined with near-surface mounted technique. Polymers, 8 (7): 1-23.

Dong, J.; Q. Wang and Z. Guan. **(2013).** Structural behavior of RC beams with external flexural and flexural shear strengthening by FRP sheets. Composite Part B, 44: 604-612.

Honestyo, A. and Ardhyananta, H. (2023a). Axial compressive behavior of bubble-size plastic straw waste FRP-confined circular concrete. International Journal on Engineering Applications, 11(2), 73–80.

Honestyo, A. and Ardhyananta, H. (2023b). Tensile Properties of Woven Plastic Straw Waste Fiber-Reinforced Polymer Composites. International Journal on Engineering Application, 11(1):11-17.

Jung, J. S.; B. Y. Lee and K. S. Lee. (2019). Experimental study on the structural performance degradation of corrosion-damaged reinforced concrete beams. Advance in Civil Engineering, 9562574.

Machmoed, S. P. and Raka, I. G. P. (2021). Performance of square reinforced concrete columns confined with innovative confining system under axial compression. International Journal of GEOMATE, 21(85), 137–144.

Machmoed, S. P. and Raka, I. G. P. (2020). Potential of new innovative confinement for square reinforced concrete columns. IOP Journal of Physics: Conference Series, 1469, 012027.

O'Farrel, K. (2018). 2016-17 Australian Plastics Recycles Survey, National Report.

Pinto, D. and Raka, I. G. P. (2019). Axial compressive behavior of square concrete columns retrofitted with GFRP straps. International Journal of Civil Engineering and Technology, 10(1), 2388–2400.

Rafani, M.; Soehardjono, A.; Wisnumurti and Wibowo, A. (2021). A theoretical study of GFRP RC beams deflection, Journal of Physics: Conference Series, 1477, 052047.

Raval, S. S. and Dave, U. V. (2013). Effectiveness of various methods of jacketing for RC beam. Procedia Engineering, 51: 230-239.

Ritch, E.; C. Brennan and C. MacLeod. (2009). Plastic bag politics: modifying consumer behaviour for sustainable development. International Journal of Consumer Studies, 33(2):168-174.

Rocha-Santos, T. and Duarte, A. C. (2015). A critical overview of the analytical approaches to the occurrence, the fate and the behavior of microplastics in the environment, TrAC Trends in Analytical Chemistry, 65:47-53.

Sabariman, B.; Soehardjono, A.; Wisnumurti and Wibowo, A. (2020). Stress-strain model for confined fiber-reinforced concrete under axial compression. Archives of Civil Engineering, 66(2), 119–133.

Tavio; Machmoed, S. P. and Raka, I. G. P. (2022). Behavior of square RC columns confined with interlocking square spiral under axial compressive loading. International Journal on Engineering Applications, 10(5), 322–335.

Tavio; Rafani, M.; Raka, I. G. P. and Ratnasari, V. (2021). Flexural capacity predictions and comparisons of GFRP reinforced beams. Journal of Physics: Conference Series, 1477, 052049.

Wahjudi, D. I. (2014). Behavior of precast concrete beam-to-column connection with U- and L-bent bar anchorages placed outside the column panel–experimental study. Procedia Engineering, 95(2014), 122–131.

.